High-Throughput Quantification of Population Dynamics using Luminescence

Malte Muetter[1,✉], **Daniel Angst**[1], **Roland Regoes**[1], **and Sebastian Bonhoeffer**[1,✉]

[1]Department of Environmental Systems Science, ETH Zürich, Universitätstrasse 16, 8092 Zürich, Switzerland

The dynamics of bacterial population decline at antibiotic concentrations above the minimum inhibitory concentration (MIC), remain poorly characterized. This is because measuring colony-forming units (CFU), the standard assay to quantify inhibition, is too slow, labour-intensive, and costly, and can be unreliable at high drug concentrations. To offer an alternative for high antimicrobial concentrations, we measured the change in light intensity from bioluminescent *Escherichia coli* over time and compared it with the change in CFU counts as a proxy for population size. Currently, luminescence assays are commonly used below the MIC, but have not yet been evaluated extensively in the super-MIC range. For 12 of the 21 antimicrobials tested, luminescence- and CFU-based rates did not differ significantly. To investigate the source of the discrepancies observed for the remaining 9 antibiotics, we introduced a size-structured population model with a continuum of cell sizes to simulate the impact of filamentation on the light signal, and complemented the findings with microscopy imaging. Discrepancies between the two rates fell into two classes. First, because light intensity tracks biomass more closely than population size, luminescence can indicate a shallower population decline when bacteria filament. Second, CFU-based estimates can indicate a steeper population decline when antimicrobial treatment reduces the number of colonies formed per viable bacterium. This effect can result from changes in clustering behaviour, physiological changes that impair culturability, or antimicrobial carry-over. With these caveats addressed, bioluminescence offers an efficient, high-throughput alternative for quantifying bacterial dynamics at super-MIC concentrations, although its suitability depends on the chosen metric (biomass vs. cell number) and on whether the antimicrobial induces filamentation or affects culturability.

bioluminescence | colony forming units | pharmacodynamics | antibiotics | time-kill curves

Correspondence: ***maltemuetter@posteo.de, seb@env.ethz.ch***

Introduction

Accurate characterization of changes in population size under treatment is essential for understanding the evolution of antibiotic resistance. Commonly, the effect of treatment on bacterial populations is quantified by pharmacodynamic (PD) curves. PD curves quantify the relationship between a wide range of drug concentrations and a corresponding rate of change of population size (net growth) ([1]). These range from no antibiotic, through sub-MIC concentrations that only reduce population growth, to super-MIC concentrations that kill bacteria and lead to a population decline.

From the theoretical side, the most common population property used to define the growth for PD-curves is the exponential rate of change in the number of living bacteria ψ_B, reflecting both division and death rates. However, other population properties, such as changes in the number of culturable bacteria or total biomass, may also be relevant, depending on the specific biological question.

In practice, PD-curves are fitted to the rate of change of a measured proxy signal such as optical density (OD), colony-forming units (CFU) or bioluminescent light intensity.

OD is a cost-effective approach that allows real time, high-throughput recording of the turbidity of a bacterial culture, without sacrificing the population. OD is positively correlated (within a certain range) to cell density. However, since OD cannot distinguish between living and dead cells, this estimate of cell density is only reliable for increasing or stable population sizes, making it unsuitable for quantifying negative rates (kill rates).

CFU assays estimate bacterial density by counting the colonies that grow on permissive agar media from plated samples. Although labor-intensive and inherently low-throughput, CFU assays remain the gold standard for measuring population size under both sub-MIC and super-MIC conditions (e.g. [1, 2]).

Luminescence assays measure the light intensity emitted by a bioluminescent bacterial culture. It is a high-throughput method used for measuring sub-MIC growth rates in real time and *in vivo* ([3–7]). However, it remains unclear whether luminescence assays can accurately capture negative growth rates at super-MIC concentrations.

While high-throughput OD and luminescence measurements at sub-MIC concentrations provide valuable insights into drug effects on growth rates, the super-MIC range is clinically more relevant. A comprehensive investigation of super-MIC population dynamics (for example, pharmacodynamics of drug combinations or resistance mutations) remains impractical, because it relies so far mostly on costly, low-throughput CFU assays.

We address this gap by evaluating whether, and to what extent, luminescence assays can reliably quantify growth rates at super-MIC concentrations. For this, we compare changes in light intensity with changes in CFU counts. Luminescence- and CFU-based rates aligned closely for some antimicrobials (e.g., colistin and amoxicillin) but diverged substantially for others (e.g., ciprofloxacin). Here, we explore the potential and limitations of both methods, identify the conditions under which they align with the rate of change of population size, and discuss their implications for studying antimicrobial effectiveness across sub-MIC and

DRAFT

super-MIC ranges.

Results

To investigate the validity of luminescence assays as a high-throughput measure for bacterial population size and its change across the entire range of antimicrobial concentrations, we compared this measure to the number of colony-forming units (CFU). Specifically, we tested whether the rates of change in light intensity, ψ_I, and CFU, ψ_{CFU}, agree for various drugs, and if not, we explored the reasons for any discrepancies.

Methodologically, we integrated the luminescence operon *luxCDABE* into *E. coli*. To minimize plasmid copy-number effects on the light emitted by a single cell (cell-specific luminosity), we excised the operon from the pCS–λ plasmid ([3]) and inserted it into the bacterial chromosome.

Light intensity is proportional to bacterial density. We first evaluated how the observed bioluminescent light intensity, I, which represents a fraction κ of the total light emitted by the culture, correlates with bacterial density. To this end, we prepared three replicate overnight cultures of bioluminescent *E. coli*, serially diluted them tenfold, and measured the light intensity for each dilution. We found that light intensity increased linearly with bacterial density for signals above approximately $20\,\mathrm{rlu}$ (Figure S1; $R^2 = 0.987$, $n = 20$, $p < 10^{-14}$), with a proportionality constant $m = 0.006\,\frac{\mathrm{rlu\,ml}}{\mathrm{CFU}}$. From this observation, we conclude that κ remains independent of bacterial density, indicating that, up to one-tenth of the stationary-phase density, high cell densities do not attenuate emitted light. Thus, provided we maintain the same luminescence plate-reader setup, we can assume κ to be constant for all subsequent analyses.

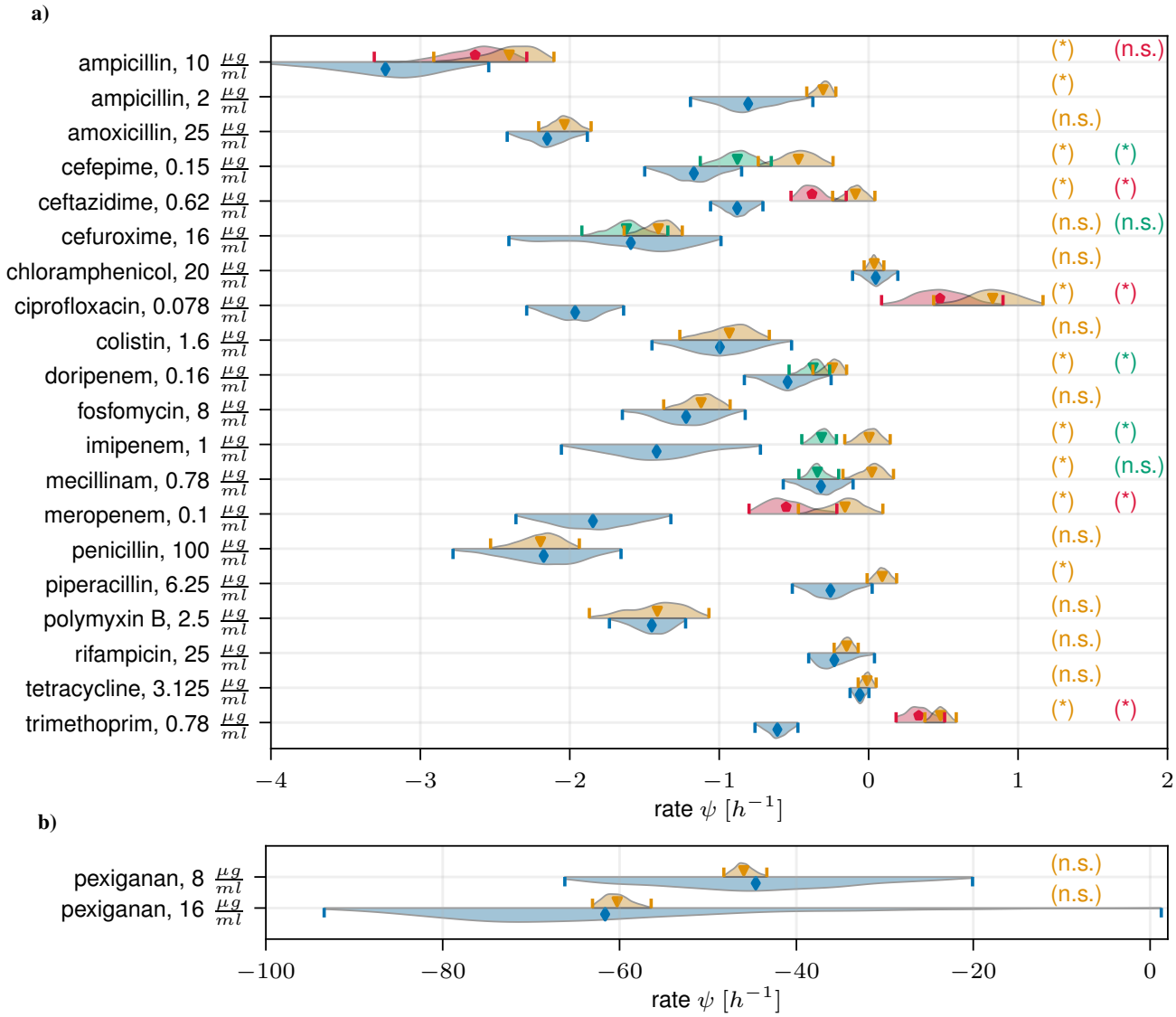

Figure 1: Comparison of CFU-based and luminescence-based rates of change. For each drug, we generated 2000 bootstrapped datasets by resampling time-series CFU and light-intensity data with replacement and fitted an exponential function to each bootstrap replicate to obtain distributions of rates. Panel (a) shows these distributions for 20 conventional antibiotics; panel (b) shows the AMP pexiganan at $8\,\frac{\mu\mathrm{g}}{\mathrm{mL}}$ and $16\,\frac{\mu\mathrm{g}}{\mathrm{mL}}$. The distribution of ψ_{CFU} is shown in blue (lower half of each violin, diamond). The distribution of ψ_I is shown in orange (upper half, triangle). Green distributions (ψ_I^*; triangle) represent luminescence-based rates calculated from data starting at the first peak onward. Red distributions show volume-adjusted luminescence rates (ψ_J; pentagon). Vertical lines mark the $95\,\%$ confidence intervals. Significance (see Methods) annotations indicate whether CFU-based rates differ significantly (*) from the corresponding luminescence-based rate or not (n.s.), with color coding matching the respective luminescence-based distribution. Wide confidence intervals for pexiganan reflect biphasic killing, steep curves, and noisy CFU data.

Luminescence-based rates agree with CFU-based kill rates for 12 out of 21 antimicrobials. Given the linearity between light intensity and bacterial density shown above, we tested whether the rate of change of light intensity ψ_I aligns with the rate of change of bacterial population size (ψ_B) under super-MIC antimicrobial concentrations. Since we cannot measure ψ_B directly, we first compared ψ_I to the CFU-based rate, ψ_{CFU}, and then discussed their relation to ψ_B. We measured CFU and light intensity over time for 21 drugs (Table S1) using an automated liquid handler (Methods) and estimated the distributions of the rates of change of CFU (ψ_{CFU}) and light intensity (ψ_I) by bootstrap (Figure 1, Table S2). We classified the luminescence and CFU-based rate distributions as "not significantly different" (n.s.) if each mean fell within the other's 95% percentile and otherwise significantly different (*). All time-series data are presented in Figures S2–S20. For amoxicillin, chloramphenicol, cefuroxime, colistin, fosfomycin, piperacillin, penicillin, pexiganan, polymyxin B, rifampicin, and tetracycline, ψ_I and ψ_{CFU} did not differ significantly. However, we observed significant discrepancies for ampicillin, cefepime, ceftazidime, ciprofloxacin, doripenem, imipenem, mecillinam, meropenem, and trimethoprim.

For all cases where significant discrepancies were observed, the light intensity declined more slowly than the CFU signal. In the following we investigate potential reasons why the light signal may decline more slowly and the CFU signal more rapidly than the "true" ψ_B.

No support for SOS-driven increase in luminescence promoter activity. To explain the observed discrepancies between CFU- and luminescence-based rates, we tested whether the SOS response might upregulate lux expression, increasing the cell-specific luminosity. To this end, we exposed the strains to UV light to induce the SOS response. Specifically, we alternated between measuring light intensity and optical density, and exposing cultures to UV (Appendix S4).

UV treatment impaired bacterial growth significantly, yet the OD-normalized light intensity (approximating cell light output) of UV-treated cells was lower than that of untreated controls (Figure S21d; t-test, $p = 3 \cdot 10^{-5}$ for the last time point). This implies that SOS induction did not upregulate lux expression, as cells under SOS had lower light output per cell than controls. While we cannot exclude the possibility that a non–UV-induced SOS response enhances cell-specific luminosity, our findings suggest that promoter upregulation is unlikely to explain why luminescence-based rates exceed CFU-based rates.

Filamentation aligns with divergence between CFU- and luminescence-based rates. Antibiotic pressure is known to impair septation and induce bacterial filamentation. Our second hypothesis was that larger, filamented cells might emit more light per cell, thereby driving the divergence between CFU- and luminescence-based rates. We explored this for a subset of the antibiotics tested by imaging bacteria before and after two hours of antibiotic treatment (Figure S22–S34; see Methods). From these images, we measured bacterial length and width (Figure S35) and calculated the cell volumes (Figure 2, Appendix S4).

For antibiotics where microscopy showed no significant filamentation (amoxicillin, colistin, fosfomycin, rifampicin, and tetracycline, Table S3), luminescence-based and CFU-based rates did not differ significantly (Figure 1, Table S2). In contrast, for those drugs where microscopy data indicated significant filamentation (ampicillin, ceftazidime, ciprofloxacin, meropenem, and trimethoprim), luminescence-based rates were significantly higher than CFU-based rates.

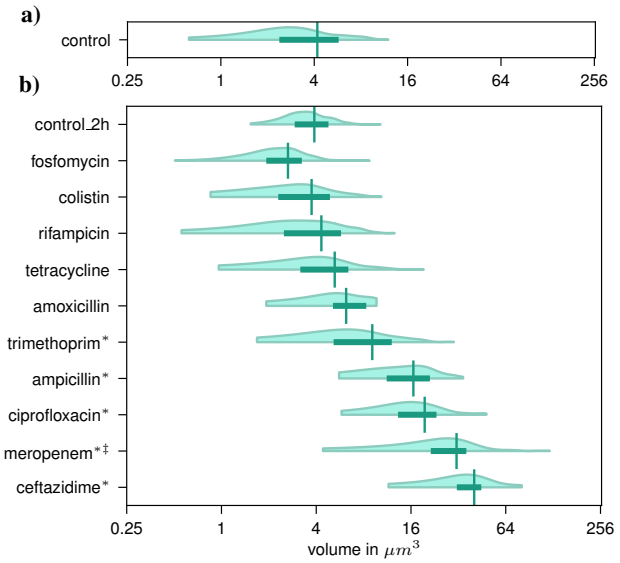

Figure 2: Density distributions (2.5–97.5% percentile range) of pooled cell volumes acquired by microscopy imaging, shown (a) before and (b) after 2 h of antibiotic treatment. Boxes indicate the 25–75 % interquartile range, and vertical bars mark the mean. Significance (*) was assessed by bootstrapping cell volumes 200 times with replacement for each replicate (image) and treatment, pooling the bootstrapped volumes by treatment, and comparing the resulting 95% confidence interval of the mean to that of the untreated control (`control_2h`). ‡ Carbapenems tend to deform cells into a lemon-like shape (Figure S30), resulting in poor fitting quality since our algorithm assumes a cylindrical geometry.

Filamentation model predicts divergence between luminescence- and CFU-based rates. To further investigate the link between filamentation and the recorded light signal, we developed a simplified population dynamical model which incorporates bacterial filamentation (Appendix S3). In this model, cells elongate linearly [8], causing the population to converge to an equilibrium cell volume, provided the division rate remains above zero (Figure S36). We assume that cell-specific luminosity scales with cell volume — i.e., the volume-specific luminosity remains constant.

We simulate filament-inducing treatment by reducing the division rate by $\Delta\lambda$, which causes an initial rapid increase in average cell size. As the mean cell volume stabilizes and cell-specific luminosity reaches equilibrium, the luminescence-based rate converges to the rate of change of population size ψ_B (Figure S36). Depending on the division and death rates, this dynamic can result in an initial peak in light intensity followed by a decline (Figure S36b).

This initial peak in light intensity, as predicted by the model, was experimentally observed for several drugs associated with filamentation (Figures S3, S5, S9, S11, S12, and S13).

To investigate the dependence of ψ_B and ψ_I on treatment-induced changes in division rate and death rate (δ), we simulated four hours of treatment (details and parameters in Appendix S3). Our model shows that a reduction in λ leads to higher luminescence-based rates ψ_I relative to the rate of change of population size ψ_B, with particularly large discrepancies when the death rate is low (Figure 3). The results from this model suggest that excluding early data points, where the mean cell volume changes rapidly, improves agreement between the estimated rates ψ_I and ψ_B. This is evident in Figure S36b, where the slopes inferred from luminescence and from population size differ initially but are nearly identical at later times.

We tested this approach by refitting all experimentally acquired luminescence-based rates that exhibited an initial peak, excluding data points recorded before the light signal reached its maximum. The resulting distributions of ψ_I^* (green) are shown in Figure 1. An exception was made for meropenem, for which we know the change of cell volume and thus applied an alternative correction as described below. This adjustment substantially reduced the difference between CFU- and luminescence-based estimates for all tested drugs and fully eliminated the discrepancy for mecillinam.

Adjusting luminescence intensities by changes in volume narrows the gap between CFU- and luminescence-based rates. Given the model-predicted differences between ψ_I and ψ_B in filamenting populations, we next tested whether combining morphological data with measured light intensities can help infer ψ_B. This approach only works if the volume-specific luminosity is constant (Appendix S2, Equation S12). We used the individual cell volume data acquired by microscopy imaging before and after treatment, $v_{\mathrm{obs},0} = 4.17\,\mu\mathrm{m}^3$ and $v_{\mathrm{obs},2\mathrm{h}}$, for all drugs that caused significant filamentation (ampicillin, ceftazidime, ciprofloxacin, meropenem, and trimethoprim). The light intensities were then volume-corrected as $J(t) = I(t)\, v_{\mathrm{obs},0}/v(t)$, where $v(t)$ is derived from the filamentation model (Eq. (S44), Appendix S3). The free parameters were determined by minimizing Equation S51. All adjusted light signals J are shown in Figures S2a, S4, S7, and S13.

For ampicillin, the CFU-based and volume-corrected luminescence-based rates (ψ_J) did not differ significantly (Table S2). For ceftazidime, ciprofloxacin, and meropenem, volume correction reduced the discrepancy, but ψ_J remained significantly above ψ_{CFU}. We observed in all experiments that volume correction narrowed but never reversed the discrepancy ($\psi_{\mathrm{CFU}} \leq \psi_J \leq \psi_I$, Equation S23). From this observation and the derivation in the SI (Appendix S2), we conclude that ψ_I is closer to ψ_V (rate of total cell volume change) than to ψ_B (rate of bacterial number change).

Three factors may explain these residual differences: (i) the assumption of constant volume-specific luminosity may not hold; (ii) the approximation of $v(t)$ may be inaccurate, and excluding entangled or overlapping cells from the analysis introduces a bias that underestimates the volume of heavily filamented cells; (iii) the CFU-based method may underestimate ψ_B.

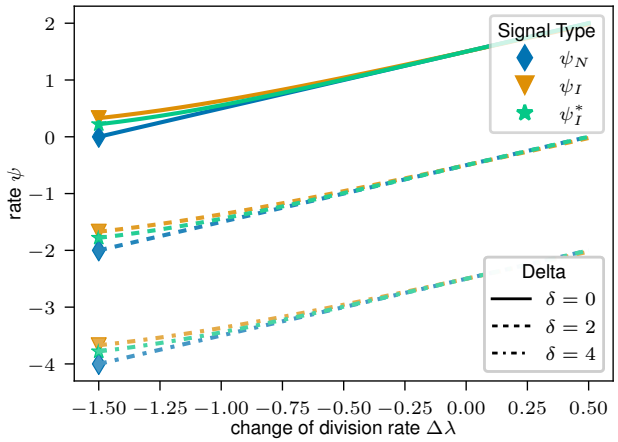

Figure 3: Simulations based on the filamentation model quantifying how changes in division rate due to treatment ($\Delta\lambda$) and death rate (δ) influence the rate of change of population size (ψ_B, blue), the rate of change of light intensity (ψ_I, orange), and the rate of change of light intensity when the first 2 hours of data are excluded (ψ_I^*, green). These illustrative simulations were conducted using an initial division rate $\lambda_0 = 1.5\,\mathrm{h}^{-1}$. More details and all parameter values can be found in Appendix S3.

For ciprofloxacin, the large disparity between ψ_{CFU} and ψ_I is unlikely to be explained by factors (i) and (ii) alone. Bringing the two rates into agreement solely by adjusting cell-specific luminosity would require an almost four-order-of-magnitude increase, which appears implausible. We therefore conclude that, in this case, CFU-based measurements likely also underestimate ψ_B (iii).

CFU-based estimates can overestimate the rate of population decline. After exploring why luminescence assays can underestimate the rate of population decline, we now explore why CFU assays may overestimate it. By definition, the rate of change of the CFU signal, ψ_{CFU}, only matches ψ_B if the number of colonies emerging per plated bacterium, $\eta \in [0, 1]$ (Equation S4), is constant over time (Appendix S2, Equation S6). This assumption can be problematic for three main reasons:

a) **Loss of culturability:** The number of colonies emerging per plated bacterium, η, depends on the division rate λ, which can be affected temporarily or permanently by treatment ([9]), e.g. due to DNA damage. In extreme cases, viable and culturable cells can be converted into viable but non-culturable (VBNC) cells ([10–12]), meaning they continue to be metabolically active but cease to divide ($\lambda = 0$) and therefore no longer form colonies on agar. Typically, cells can reproduce at the start of a time-kill assay but may, depending on the drug, partially or completely lose this ability as the assay progresses, causing an underestimation of ψ_B.

b) **Antimicrobial carryover:** Antibiotics transferred onto agar by plating a diluted culture can experience a residual treatment effect; either on the division rate λ or the death rate δ, depending on the mode of action of the drug and thus reduce the probability of colony formation. This phenomenon, known as antimicrobial carryover, has been described in previous studies [13–15]. Its effect is usually minimal at the start of a time-kill assay, when bacte-

rial density is high and plated samples are highly diluted. However, as the assay progresses and bacterial density declines, less dilution is needed, increasing the concentration of the transferred antibiotic. As a consequence, CFU-based rates would underestimate ψ_B between two time points t_0 and t_1 by $\frac{\ln(\eta_1)-\ln(\eta_0)}{\Delta t}$, where η_i denotes the mean number of colonies formed per plated bacterium at time t_i.

c) **Aggregation:** Filamentation or altered cell adhesiveness can change the size distribution of colony-initiating clusters on agar after plating (Equation S3). Changes in cluster size in turn, affect the average number of clusters per plated bacterium, thereby biasing estimates of ψ_B.

Partial loss of culturability causes CFU to underestimate ψ_B for ciprofloxacin and trimethoprim treatment During ciprofloxacin treatment, CFU counts fell steeply while light intensity continued to rise (Figure S7), prompting us to investigate whether these results could be confirmed visually at the single-cell level. To this end, we plated treated cultures on phosphate-buffered saline (PBS) agar containing propidium iodide (PI). PI is a red fluorescent dye that binds to nucleic acids and is widely used to stain permeable cells due to its inability to penetrate intact cell membranes. Microscopic imaging (Figure S27) revealed almost no red fluorescence, indicating that the cells remained impermeable. Although impermeability alone does not confirm viability, additional observations support the conclusion that most cells were still alive: the absence of bacterial debris (as has been observed for drugs with similar decline in CFU such as amoxicillin), visible growth indicated by increased cell size compared to two hours earlier, and continued (and even increased) light emission. These findings suggest that most cells remain alive but are unable to form colonies under the provided conditions, possibly due to DNA damage induced by ciprofloxacin [16]. This observation aligns well with previous studies on ciprofloxacin, which found that CFU can underestimate viability relative to non-culture-based methods [10, 17].

Trimethoprim treatment showed similar, though less pronounced, results (Figure S19). Trimethoprim, which impairs DNA replication ([18]), likewise caused an increase in light intensity and a decline in CFU counts, while microscopy revealed intact, mostly impermeable, filamented cells (Figure S34).

Antimicrobial carryover causes underestimation of ψ_B for pexiganan using CFU. Building on our understanding of when luminescence assays accurately estimate ψ_B, we hypothesized that antimicrobial peptides (AMPs) would be an ideal application for this method. We expected that, during the AMP's short killing phase, changes in the cell-specific luminosity would remain negligible compared to the high kill rates AMPs can achieve.

Initially, however, we failed to recover almost any colonies on agar, despite the light intensity indicating a high enough bacterial density. Moreover, colony counts were inconsistent across dilutions: wells diluted 100-fold and 1000-fold from the same time point yielded similar colony numbers, instead of reflecting the tenfold difference. We suspected that AMPs from the liquid culture, including those attached to the bacterial surface, were carried over into the PBS dilution medium, causing continued cell death during dilution and after plating. To test this, cultures treated with pexiganan for $1\,\mathrm{min}$ were diluted 1:100 in PBS and subsequently sampled and plated at four time points, approximately 45 minutes apart. As dilution medium, we tested PBS supplemented with various concentrations of $CaCl_2$ and $MgCl_2$. These compounds were selected based on prior evidence that they inhibit the activity of other AMPs ([19]).

Our results show that supplementing the dilution medium increased the measured CFU substantially (Figure S38, Appendix S4). This indicates that bacterial survival probability increases when diluted in the supplemented medium. Conversely, diluting in unsupplemented PBS does not stop bacteria from dying. Supplementing $100\,\mathrm{mM}$ $MgCl_2$ yielded the highest CFU count for the first time point (Table S4). Since CFU cannot systematically overestimate bacterial density, this count represents the best estimate of the bacterial density. Consequently, we supplemented the PBS with $100\,\mathrm{mM}$ $MgCl_2$ in subsequent pexiganan experiments.

Given this insight into the residual killing effect of pexiganan and how to mitigate it, we repeated the CFU time-kill experiment using two different dilution media (Appendix S4). We recorded three replicates for each of the two time-kill curves. We diluted the cultures at each time point in either pure PBS or PBS supplemented with $100\,\mathrm{mM}$ $MgCl_2$ and counted colonies on all agar plates from three dilution steps. To lower the detection limit by one order of magnitude, we increased the plated volume from $10\,\mu\mathrm{L}$ to $100\,\mu\mathrm{L}$. Since this volume exceeds the capacity of the automated high-throughput setup, we used the standard manual CFU plating method instead.

We observed a much steeper initial decline in CFU for the cultures diluted in pure PBS compared to the supplemented ones (Figure S39). In pure PBS, more highly diluted samples consistently yielded higher CFU estimates (Figure S39a), supporting the antimicrobial carryover hypothesis. This pattern diminished over time, suggesting a reduction in the residual killing effect of pexiganan, which we discuss below.

Luminescence and CFU show identical decline rates for pexiganan time-kill curves if residual killing is prevented. To confirm that eliminating residual pexiganan killing aligns CFU and luminescence, we supplemented PBS with $100\,\mathrm{mM}$ $MgCl_2$ and measured both signals at pexiganan concentrations of $8\,\frac{\mu\mathrm{g}}{\mathrm{mL}}$ and $16\,\frac{\mu\mathrm{g}}{\mathrm{mL}}$ using the "rapid luminescence-CFU assay setup" (Methods). We observed no significant difference between the CFU- and luminescence-based rates for either of the tested pexiganan concentrations (Figure 1b, Table S2). However, examining the time series (Figure S20) revealed that while CFU and luminescence signals declined in parallel for the $8\,\frac{\mu\mathrm{g}}{\mathrm{mL}}$ treatment, they diverged for the $16\,\frac{\mu\mathrm{g}}{\mathrm{mL}}$ kill curve. In this case, the CFU signal initially declined much faster (rates below $-200\,\mathrm{h}^{-1}$), and subsequently declined more slowly than the corresponding luminescence signal, ultimately resulting in a similar average rate (approxi-

mately $-60\,\mathrm{h}^{-1}$).

This pattern suggests that luminescence assays may not be able to capture extremely rapid kill rates, potentially due to short delays between irreversible cell damage, actual cell death, and the subsequent cessation of luminescence. This limitation should not affect measurements for most conventional antibiotics, for which rates rarely exceed $-10\ \mathrm{h}^{-1}$.

Pexiganan rapidly loses killing capacity. During the pexiganan experiments, we observed an initial steep decline in bacterial density, predicted by both CFU and luminescence, followed by almost constant signals (Figures S20, S39). Two possible, non-exclusive explanations for this observation are: first, pexiganan is deactivated or sequestered from the medium by attaching to targets on the bacteria over time; and second, the remaining bacteria are unaffected by the AMP because they are resistant or persisters. To investigate the first explanation, we exposed bacteria to pexiganan for $5\,\mathrm{min}$ at $16\,\frac{\mathrm{\mu g}}{\mathrm{mL}}$, after which the supernatant was collected and tested for its ability to kill bacteria (Appendix S4). While the initial treatment showed rapid bacterial killing ($\psi_{\mathrm{CFU}} \approx -46\,\mathrm{h}^{-1}$ between $t_0 = 0$ and $t_1 = 5\,\mathrm{min}$), bacteria exposed to the supernatant alone showed no significant reduction in viability (Figure S40, Table S5). These results show that the supernatant has no residual killing effect. This makes deactivation or sequestration through attachment of pexiganan the likely explanation for the flattening CFU signal, even though we did not assess whether the surviving cells are resistant or persisters.

Discussion

We evaluated whether luminescence can serve as a high-throughput proxy for population dynamics by comparing it with CFU assays. We found no significant difference between CFU- and luminescence-based rates for treatments that neither induce substantial changes in culturability nor provoke strong morphological changes, such as filamentation. However, for drugs that induce filamentation and/or loss of culturability, the two methods can yield significantly different results. The divergence between the two rates does not imply that either method is incorrect; rather, each captures a different aspect of the population.

The CFU method counts bacteria capable of forming colonies on permissive media (i.e., culturable cells). When inferring growth rates from CFU, the observed rate of change ψ_{CFU} reflects both the rate of change of population size ψ_B and changes in the probability that a plated bacterium forms a colony, η (Equation S4). The CFU-based rate equals ψ_B only if η remains constant over time.

However, η can change for three main reasons. First, altered clustering behavior can change how many bacteria seed a single colony. This directly shifts the observed colony count. Second, physiological changes to the bacteria may lead to a long-term or permanent change in culturability ([9–12, 17, 20]), which may increase the fraction of viable cells that fail to form colonies, e.g. due to a reduced division rate. Third, residual drug activity carried over to the agar can alter on-plate conditions, thereby reducing division or increasing the death rate ([13–15]).

Preventing antibiotic carryover when handling low-density cultures treated with highly concentrated antimicrobials is challenging and, in some cases, infeasible. Centrifugation-based washing (pelleting bacteria and replacing the supernatant) can remove residual drug, but only if the processing delay is negligible relative to the antibiotic's killing kinetics — a condition unlikely to hold for fast-acting agents such as pexiganan. Moreover, although bacteria generally tolerate high centrifugal forces ([21]), the impact on compromised cells, such as those with destabilized walls, is unknown. As an alternative, we found that supplementing the dilution medium with $MgCl_2$ effectively neutralizes residual AMP activity, preventing residual killing effects in CFU assays for pexiganan. However, this strategy is not generalizable, as for most antimicrobials the deactivating agents are unknown — or may not even exist. For these cases, it is impossible to accurately derive ψ_B from CFU counts at high drug concentrations.

In contrast to CFU assays, luminescence assays become more reliable at high, fast-killing concentrations. This is because ψ_I reflects both the rate of population size change, ψ_B, and changes in cell-specific luminosity (Equation S9); when population declines rapidly, ψ_I converges to ψ_B. One exception was observed for extremely rapid kill rates (exceeding $-60\,\mathrm{h}^{-1}$), as seen for highly concentrated pexiganan, likely due to short delays between cell death and cessation of luminescence.

For lower kill rates, we observed that the absence of filamentation was a good indicator of stable cell-specific luminosity. In cases where drugs induced filamentation, CFU- and luminescence-based rates diverged. We further demonstrated that correcting for the increased cell size partly compensates for the difference between CFU- and luminescence-based estimates, and we found that the rate of change in light intensity is closer to the change in total cell volume than to the change in total cell number (Appendix S2). This makes a constant volume-specific (or mass-specific) luminosity a better assumption than a constant cell-specific luminosity.

Changes in both CFU and luminescence are used as proxy signals for population net growth rates ([1–7]). Whether discrepancies between the changes in these proxy signals and the changes in living bacteria pose a problem depends on the underlying biological question. The rate of change of living bacteria, ψ_B, is most commonly applied in theoretical modeling to create predictions, making its estimation important. If, instead, the aim is to assess a population's reproductive potential, for example, in studies focusing on evolutionary dynamics, examining changes in the number of culturable cells (as approximated by CFU) may be more relevant than ψ_B, as only culturable cells contribute to subsequent generations and thus to evolution. Additionally, tracking changes in total biomass (closer to ψ_I) can be more relevant than the number of living bacteria, as biomass accounts for a potential "catch-up" effect, whereby filamented cells fragment into multiple viable units once antibiotic pressure is removed ([20, 22]).

A notable challenge of using luminescence assays is the absence of a fundamental biological principle linking cell-specific luminosity uniquely to a single biological property, such as biomass, cell number, or gene copy number. We therefore recommend applying luminescence-based methods primarily over short to intermediate timescales, during which abiotic conditions remain relatively stable. When the impact of treatment on cell size is unknown, one should assume that ψ_I primarily reflects the rate of change of biomass rather than cell number. Thus, to reliably estimate ψ_B, it is essential to ensure either that cells do not filament, correct for changes in mean cell volume, or restrict analyses to intervals during which volume changes are minimal relative to population decline. Finally, because most drugs in this study were tested at only one concentration, the generalizability of our drug-specific findings remains to be shown.

Our results show that neither CFU nor luminescence is optimal for every experimental scenario. Instead, CFU and luminescence work best under different conditions, measure different population properties and complement each other well. At low and intermediate drug concentrations, changes in CFU accurately reflect changes in bacterial density, but CFU becomes unreliable at high drug concentrations.

Luminescence, by contrast, becomes more reliable at high concentrations, where CFU becomes unreliable. In practice, the luminescence method significantly reduces labor, consumables, and costs: eight PD curves with twelve concentrations and four replicates each can be fit on a single 384-well plate, whereas measuring CFU would require more than 8,000 agar plates, hundreds of dilution plates, and substantial manual labor. Given their scalability and cost-effectiveness, luminescence assays offer a valuable alternative for high-throughput analysis, particularly at high antimicrobial concentrations, where traditional methods become unreliable or even unusable.

Methods

Strains We generated a bioluminescent strain by integrating the luxCDABE operon, driven by the constitutive $\lambda - Pr$ promoter, and a kanamycin resistance cassette (as a marker) into the chromosome of *Escherichia coli* MG1655. This integration replaced the galK gene and was achieved using λ-Red recombination ([23]), following a protocol by Hughes [24, 19–26]. The integrated elements were derived from the pCS-λ plasmid ([3]). Primers are listed in Table S6. For all time-course experiments, we prepared three replicate exponential cultures by diluting overnight cultures (grown for approximately 18 hours) 1:100 and growing them to exponential phase for 1–1.5 hours.

Media We used LB (Sigma L3022) as a liquid medium and, as a solid medium for CFU plating, LB with $1.5\,\%$ agar. Cultures were treated by diluting the tenfold working concentration of one of 21 antimicrobials 1:10 (Table S1). Phosphate-buffered saline (PBS, Sigma 79383) was used as the diluent for CFU assays. If cultures were treated with pexiganan, $100\,\mathrm{mM}$ $MgCl_2$ was added. For microscopy, we added $1\,\frac{\mu g}{mL}$ propidium iodide (PI) to the liquid medium and used PBS/PI agar plates (containing PBS with $1.5\,\%$ agar and $1\,\frac{\mu g}{mL}$ PI) as solid medium.

Automated CFU plating. We automated the high-throughput colony-count method described by [25] using an Evo 200 liquid-handling platform (Tecan) integrated with a Liconic STX100 incubator. The platform handles liquids and automatically moves, images, and incubates plates. We produced six colony streaks by spotting six $10\,\mu L$ drops of diluted bacterial culture onto a one-well agar plate. Plates were automatically tilted for $7\,s$ on a custom-built tilter integrated into the handling platform, to spread the drops and distribute the bacteria. After incubation, plate images were captured using the Pickolo camera (SciRobotics).

The platform is controlled by custom-generated worklists executed in the native software "Evoware". These worklists were generated using the Python package `pypetting` (version 1.0.1). We analyzed the captured images of the agar plates using a custom colony-recognition script that automatically identifies colonies and allowed the manual addition of unidentified colonies and the removal of mismatched ones. All Python classes for generating the worklists and analyzing colonies are available at Zenodo (DOI: 10.5281/zenodo.15261184).

Luminescence measurements. To record the luminescent light intensity, we used an Infinite F200 spectrophotometer plate reader (Tecan), which is also integrated into the liquid-handling platform, with an exposure time of one second. We set $20\,\mathrm{rlu}$ as the lower detection limit and excluded all data points below.

Luminescence-CFU assay setup. To measure the CFU and light intensity at seven time points, we treated the exponential cultures and then distributed them onto seven (one for each time point) white 384-well plates (Greiner, 781073), with each culture well containing $54\,\mu L$ medium and $6\,\mu L$ 10x stock solution. We adjusted the duration of the experiments between two and five hours, depending on the anticipated kill rate. For each time point, an assay plate was transferred from the incubator to the plate reader for luminescence measurement. Subsequently, a dilution series was conducted directly in the white plate and plated using the automated plating method, after which the plate was discarded.

Rapid luminescence-CFU assay setup. This experiment is a variation of the *Luminescence-CFU assay setup*, adjusted to measure rapid kill curves for the antimicrobial peptide pexiganan. In this setup, we captured four time points within $5\,\mathrm{min}$. Cultures were treated in a 96-deep-well plate (Greiner, 780285) by adding $100\,\mu L$ of the 10x stock solution to $900\,\mu L$ exponential phase culture. $60\,\mu L$ of the treated culture was then transferred to a 384-well white plate (Greiner, 781073) and placed in the plate reader for continuous luminescence recording. For the four CFU time points, samples were taken directly from the deep-well plate, automatically diluted in a 96-well plate (Greiner, 655101) to halt the antimicrobial activity and then plated.

Morphology experiments. To assess treatment-induced morphological changes, we imaged treated (for 2 hours) and untreated bacteria by spotting 2 µL droplets onto PBS/PI-agar plates. The spots were cut out and flipped onto Ibidi μ-dishes (Ibidi, 80136) for imaging. We used an Eclipse Ti2 microscope (Nikon) with a 100x objective connected to a DS-Qi2 Nikon Scientific CMOS (sCMOS) camera to image the bacterial cells. The microscope setup included an additional 1.5x zoom, which was used only for some images due to unintentional variation. We estimated the width and length of the bacterial cells using a custom Python script, as described in Appendix S4.

Fitting rates of change ψ. To compare the rates of change of two signals, we first excluded all data below the detection limits (empty plates or light intensity below 20 rlu). We then truncated both signals at the latest time point where both remained above the detection limit, ensuring the same time frame was used for comparison. Next, we bootstrapped 200 datasets with replacement per signal, while ensuring that each dataset contained more than one time point For each dataset, we applied a simple regression to fit an exponential function to all time points of each time-kill curve resulting in distributions with 200 rate estimates each.

Significance. We classify two distributions of rates as not significantly different (n.s.) if the mean of each distribution falls within the 95% confidence interval of the other. Otherwise, we classify them as significantly different (*).

Data, Materials, and Software Availability

Experimental datasets are available at Zenodo (DOI: 10.5281/zenodo.15261454). Analysis scripts, plate-handling worklists, colony-recognition code, and model code are available at Zenodo (DOI: 10.5281/zenodo.15261184).

Acknowledgements

We thank Marco La Fortezza and Ricardo León Sampedro for assistance with microscopy imaging. During manuscript preparation, we used OpenAI's ChatGPT for editorial assistance (grammar, phrasing, and proofreading). This work was supported by funding from ETH Zurich.

Bibliography

1. Roland R. Regoes, Camilla Wiuff, Renata M. Zappala, Kim N. Garner, Fernando Baquero, and Bruce R. Levin. Pharmacodynamic functions: A multiparameter approach to the design of antibiotic treatment regimens. *Antimicrob. Agents Chemother.*, 48(10):3670–3676, 2004. ISSN 00664804. doi: 10.1128/AAC.48.10.3670-3676.2004.
2. Sunniva Foerster, Magnus Unemo, Lucy J. Hathaway, Nicola Low, and Christian L. Althaus. Time-kill curve analysis and pharmacodynamic modelling for in vitro evaluation of antimicrobials against Neisseria gonorrhoeae. *BMC Microbiol.*, 16(1):1–11, 2016. ISSN 14712180. doi: 10.1186/s12866-016-0838-9. URL http://dx.doi.org/10.1186/s12866-016-0838-9.
3. Roy Kishony and Stanislas Leibler. Environmental stresses can alleviate the average deleterious effect of mutations. *J. Biol.*, 2(2):1–10, 2003. ISSN 14785854. doi: 10.1186/1475-4924-2-14.
4. Pamela Yeh, Ariane I. Tschumi, and Roy Kishony. Functional classification of drugs by properties of their pairwise interactions. *Nat. Genet.*, 38(4):489–494, 2006. ISSN 10614036. doi: 10.1038/ng1755.
5. Remy Chait, Allison Craney, and Roy Kishony. Antibiotic interactions that select against resistance. *Nature*, 446(7136):668–671, 2007. ISSN 14764687. doi: 10.1038/nature05685.
6. Bor Kavčič, Gašper Tkačik, and Tobias Bollenbach. Mechanisms of drug interactions between translation-inhibiting antibiotics. *Nat. Commun.*, 11(1), 2020. ISSN 20411723. doi: 10.1038/s41467-020-17734-z.
7. S Andreas Angermayr, Tin Yau Pang, Guillaume Chevereau, Karin Mitosch, Martin J Lercher, and Tobias Bollenbach. Growth-mediated negative feedback shapes quantitative antibiotic response. *Mol. Syst. Biol.*, 18(9):1–19, 2022. ISSN 1744-4292. doi: 10.15252/msb.202110490.
8. Ping Wang, Lydia Robert, James Pelletier, Wei Lien Dang, Francois Taddei, Andrew Wright, and Suckjoon Jun. Robust growth of escherichia coli. *Curr. Biol.*, 20(12):1099–1103, 2010. ISSN 09609822. doi: 10.1016/j.cub.2010.04.045. URL http://dx.doi.org/10.1016/j.cub.2010.04.045.
9. Harry Eagle and Arlyne D Musselman. the slow recovery of bacteria from the toxic effects of penicillin. *J. Bacteriol.*, 58:475–490, 1949. doi: 10.1128/jb.58.4.475-490.1949. URL https://journals.asm.org/journal/jb.
10. Valérie Besnard, Michael Federighi, Eric Declerq, Florence Jugiau, and Jean Michel Cappelier. Environmental and physico-chemical factors induce VBNC state in Listeria monocytogenes. *Vet. Res.*, 33(4):359–370, jul 2002. ISSN 09284249. doi: 10.1051/vetres:2002022. URL http://dx.doi.org/10.1051/vetres:2002022.
11. James D. Oliver. The viable but nonculturable state in bacteria. *J. Microbiol.*, 43 Spec No: 93–100, feb 2005. ISSN 1225-8873. URL https://pubmed.ncbi.nlm.nih.gov/15765062/.
12. Laam Li, Nilmini Mendis, Hana Trigui, James D. Oliver, and Sebastien P. Faucher. The importance of the viable but non-culturable state in human bacterial pathogens. *Front. Microbiol.*, 5(JUN):1–1, 2014. ISSN 1664302X. doi: 10.3389/fmicb.2014.00258.
13. R. D. Pearson, R. T. Steigbigel, H. T. Davis, and S. W. Chapman. Method for reliable determination of minimal lethal antibiotic concentrations. *Antimicrob. Agents Chemother.*, 18(5):699–708, 1980. ISSN 00664804. doi: 10.1128/AAC.18.5.699.
14. R. H.K. Eng, S. M. Smith, C. E. Cherubin, and E. N. Tan. Evaluation of two methods for overcoming the antibiotic carry-over effect. *Eur. J. Clin. Microbiol. Infect. Dis.*, 10(1):34–38, 1991. ISSN 09349723. doi: 10.1007/BF01967095.
15. Jessica Coates, Bo Ryoung Park, Dai Le, Emrah Şimşek, Waqas Chaudhry, and Minsu Kim. Antibiotic-induced population fluctuations and stochastic clearance of bacteria. *Elife*, 7:1–26, 2018. ISSN 2050084X. doi: 10.7554/eLife.32976.
16. Cindy Levine, Hiroshi Hiasa, and Kenneth J. Marians. DNA gyrase and topoisomerase IV: Biochemical activities, physiological roles during chromosome replication, and drug sensitivities. *Biochim. Biophys. Acta - Gene Struct. Expr.*, 1400(1-3):29–43, 1998. ISSN 01674781. doi: 10.1016/S0167-4781(98)00126-2.
17. Renfei Wu, Cong Li, Jiuyi Li, Jelmer Sjollema, Gésinda I. Geertsema-Doornbusch, H. Willy de Haan-Visser, Emma S.C. Dijkstra, Yijin Ren, Zexin Zhang, Jian Liu, Hans C. Flemming, Henk J. Busscher, and Henny C. van der Mei. Bacterial killing and the dimensions of bacterial death. *npj Biofilms Microbiomes 2024 101*, 10(1):1–8, sep 2024. ISSN 2055-5008. doi: 10.1038/s41522-024-00559-9. URL https://www.nature.com/articles/s41522-024-00559-9.
18. Richard Gleckman, Noel Blagg, and Dennis W. Joubert. Trimethoprim: Mechanisms of Action, Antimicrobial Activity, Bacterial Resistance, Pharmacokinetics, Adverse Reactions, and Therapeutic Indications. *Pharmacother. J. Hum. Pharmacol. Drug Ther.*, 1(1):14–19, 1981. ISSN 18759114. doi: 10.1002/j.1875-9114.1981.tb03548.x.
19. Berthony Deslouches, Kazi Islam, Jodi K. Craigo, Shruti M. Paranjape, Ronald C. Montelaro, and Timothy A. Mietzner. Activity of the de novo engineered antimicrobial peptide WLBU2 against Pseudomonas aeruginosa in human serum and whole blood: Implications for systemic applications. *Antimicrob. Agents Chemother.*, 49(8):3208–3216, 2005. ISSN 00664804. doi: 10.1128/AAC.49.8.3208-3216.2005.
20. F. Baquero, E. Culebras, C. Patron, J. C. Pérez-Díaz, J. C. Medrano, and M. F. Vicente. Postantibiotic effect of imipenem on gram-positive and gram-negative micro-organisms. *J. Antimicrob. Chemother.*, 18 Suppl E(SUPPL. E):47–59, 1986. ISSN 0305-7453. doi: 10.1093/JAC/18.SUPPLEMENT_E.47. URL https://pubmed.ncbi.nlm.nih.gov/3546247/.
21. Shigeru Deguchi, Hirokazu Shimoshige, Mikiko Tsudome, Sada Atsu Mukai, Robert W. Corkery, Susumu Ito, and Koki Horikoshi. Microbial growth at hyperaccelerations up to 403,627 x g. *Proc. Natl. Acad. Sci. U. S. A.*, 108(19):7997–8002, may 2011. ISSN 00278424. doi: 10.1073/PNAS.1018027108. URL https://www.pnas.org/doi/abs/10.1073/pnas.1018027108.
22. Julien Cayron, Annick Dedieu-Berne, and Christian Lesterlin. Bacterial filaments recover by successive and accelerated asymmetric divisions that allow rapid post-stress cell proliferation. *Mol. Microbiol.*, 119(2):237–251, feb 2023. ISSN 13652958. doi: 10.1111/MMI.15016.
23. Kirill A. Datsenko and Barry L. Wanner. One-step inactivation of chromosomal genes in Escherichia coli K-12 using PCR products. *Proc. Natl. Acad. Sci. U. S. A.*, 97(12):6640–6645, jun 2000. ISSN 00278424. doi: 10.1073/PNAS.120163297. URL www.pnas.orgcgidoi10.1073pnas.120163297.
24. Diarmaid Hughes, Beth Lazazzera, and Fitnat Yildiz. Experiments in Bacterial Genetics, 2013.
25. Bradley D. Jett, Kenneth L. Hatter, Mark M. Huycke, and Michael S. Gilmore. Simplified agar plate method for quantifying viable bacteria. *Biotechniques*, 23(4):648–650, 1997. ISSN 07366205. doi: 10.2144/97234BM22.